Simulations of Spinodal Nucleation in Systems with Elastic Interactions

C. J. Gagne,[1] Harvey Gould,[1] W. Klein,[2,*] T. Lookman,[2] and A. Saxena[2]
[1]*Department of Physics, Clark University, Worcester, Massachusetts 01610, USA*
[2]*Theoretical Division, Los Alamos National Laboratory, Los Alamos, New Mexico 87545, USA*
(Received 12 September 2004; published 22 August 2005)

Systems with long-range interactions quenched into a metastable state near the pseudospinodal exhibit nucleation that is qualitatively different from classical nucleation near the coexistence curve. We observe nucleation droplets in Langevin simulations of a two-dimensional model of martensitic transformations and determine that the structure of the nucleating droplet differs from the stable martensite structure. Our results, together with experimental measurements of the phonon dispersion curve, allow us to predict the nature of the droplet. The results have implications for nucleation in many solid-solid transitions and the structure of the final state.

DOI: 10.1103/PhysRevLett.95.095701 PACS numbers: 64.60.Qb, 05.10.−a, 05.70.Jk, 81.30.Kf

An outstanding challenge in solid-solid phase transformations is to understand the nucleation and growth of the transformed phase in strain based materials such as martensites, ferroelectrics, and multiferroics. Although classical nucleation theory has been invoked to describe nucleation phenomena in these materials [1–6], it is possible that the presence of long-range elastic forces greatly influences the probability of nucleation and subsequent growth that determines processing and material behavior. For example, the transformation susceptibility determined by nucleation is one of the basic factors for the hardenability of steels. Even though heterogeneous nucleation, which is sensitive to the distribution of appropriate structures in the parent phase from which product phase nuclei may be triggered, has long been considered important for martensites [7], homogeneous nucleation also has been observed if the transformational driving force is sufficiently large. However, because of the difficulty of experimentally determining nucleation droplet structure in martensites [1], little is known quantitatively about the morphology of the nucleating droplet or ''embryo,'' including its size distribution or nucleation rate for homogeneous or heterogeneous nucleation. The aim of this work is to probe for the first time the nature of the nucleating droplet and associated fluctuations by performing mesoscale simulations using realistic nonlinear models for martensites. We find that the classical theory does not accurately describe the structure of the nucleating droplet, but that concepts associated with nucleation near a spinodal [8,9] account for the observed droplet morphology. Our work also provides the basis for investigating nucleation in systems where long-range elastic forces crucially determine the morphology.

Long-range elastic interactions are important in strain based materials, such as martensites, and result from the requirement of compatibility of strain components that is necessary to preserve the continuity of the elastic media [10,11]. We refer to systems with long-range interactions as near-mean field, and use several characteristics of mean-field theory to study nucleation in these systems. Mean-field systems have a well-defined spinodal, the limit of metastability; near-mean-field systems have a pseudospinodal, which becomes better defined as the range of interaction increases [12].

Spinodal nucleation, i.e., nucleation close to the pseudospinodal, is predicted to produce a ramified droplet with a small amplitude [8,9]. The droplet need not have the same structure as the stable phase [13,14], unlike in classical nucleation where the droplet is compact and has the same structure as the stable phase [15]. Spinodal nucleation has been observed in molecular dynamic simulations of simple models [16,17], but its predictions have not been tested on more realistic representations of materials such as martensites.

We model a martensitic transformation using a Ginzburg-Landau free energy [10,11,13]:

$$F[\phi] = F_0 + F_{\rm grad} + F_{\rm cs}, \tag{1a}$$

$$F_0 = \int_0^L d^2r[\tau\phi^2 - 2\phi^4 + \phi^6], \tag{1b}$$

$$F_{\rm grad} = \int_0^L d^2r\left[\frac{a}{4}(\nabla\phi)^2 + \frac{b}{8}(\nabla^2\phi)^2\right], \tag{1c}$$

$$F_{\rm cs} = \int_0^L d^2r\left[\frac{A_1}{2}e_1^2 + \frac{A_2}{2}e_2^2\right] \tag{1d}$$

$$\approx \int_0^L d^2r d^2r' U(\vec{r} - \vec{r}')e^{-|\vec{r}-\vec{r}'|/R}\phi(\vec{r})\phi(\vec{r}'), \tag{1e}$$

where ϕ is the deviatoric strain, e_1 is the compressional strain, e_2 is the shear strain, $U(\vec{\rho} = \vec{r} - \vec{r}')$ is the Fourier transform of

$$\hat{U}(\vec{k}) = \frac{A_1}{2}\frac{(k_x^2 - k_y^2)^2}{[k^4 + 8\frac{A_1}{A_2}k_x^2k_y^2]}, \tag{2}$$

$\tau = (\theta - \theta_c)/(\theta_0 - \theta_c)$, θ is the dimensionless temperature, θ_c is the critical temperature where the $\phi = 0$ austenite minimum of F_0 disappears, θ_0 is the temperature where the three minima of F_0 are degenerate, and R is the range of the interaction. For metals R is quite large. The quantity $F_{\rm cs}$ can be written as nonlocal surface and bulk

terms in ϕ by using the St. Venant compatibility equations [10]. If we ignore defects, the bulk term kernel in k space is given by Eq. (2), $\sim 1/r^2$, and vanishes at $k_x = \pm k_y$. In the limit of a sharp surface boundary, the surface term $\sim 1/r$, and the energetic competition between this term and $F_{\rm grad}$ determines the twin width $\sqrt{L}$ [18]. As in Ref. [13], an exponential cutoff has been added to $U(\vec{\rho})$ in $F_{\rm cs}$ to simulate defects and the surface has been given a more realistic width. If the width of the interface of the droplet scales as the correlation length ξ, the surface term can be neglected for long-range interactions near the spinodal $\xi \gg R$ [13,19]. All variables are dimensionless and scaled, as we describe in detail.

We use overdamped Langevin dynamics so the equation of motion for ϕ is

$$\frac{\partial \phi(\vec{r}, \vec{t})}{\partial t} = -\frac{\delta F[\phi(\vec{r}, t)]}{\delta \phi(\vec{r}, t)} + \zeta(\vec{r}, t), \tag{3}$$

where the Gaussian noise ζ is related to the dimensionless temperature θ by the fluctuation-dissipation relation,

$$\langle \zeta(\vec{r}, t)\zeta(\vec{r}', t')\rangle = 2\theta\delta^2(r - r')\delta(t - t'). \tag{4}$$

Several predictions have been made [13] for the critical droplet when the system is quenched to just above the spinodal τ_s, with $\Delta\tau = \tau - \tau_s \ll 1$. Near-mean-field theory is applicable when the fluctuations about the mean of the order parameter are much less than the mean, i.e., when the Ginzburg parameter $G \approx \langle\phi\rangle^2/\langle\phi^2\rangle \gg 1$. We can replace $\langle\phi^2\rangle$ by $\theta\chi = \theta\partial\phi/\partial\sigma$, where χ is the zero-stress isothermal susceptibility and the stress σ is the conjugate field to the order parameter strain. Spatial averages are approximated using the appropriate power of the correlation length. The nucleation barrier in $d = 2$ is proportional to $G \approx \xi^2\phi^2/(\theta\chi) \approx \xi^2\phi^2/(\theta_c\chi) \gg 1$ [13], where $\chi \approx 2/\Delta\tau$. Because $\phi \approx \sqrt{\Delta\tau/4} \ll 1$, the droplet is difficult to distinguish from the metastable background. For $a > 0$, $\xi \approx \sqrt{a/(4\Delta\tau)}$ and $\tau_s = 0$ [13], so $G \approx a\tau/(8\theta_c)$. If $a < 0$, $\xi \approx \sqrt{|a|/(2\Delta\tau)}$ and $\tau_s = |a|^2/(8b)$, so $G \approx |a|\Delta\tau/(4\theta_c)$. The droplet is predicted to be modulated at the largest (real) value of the wave number k_0 at which the structure function [20] $S(k) \approx [\tau \pm |a|k^2/4 + bk^4/8 + \tilde{U}(k)]^{-1}$ diverges. If $a > 0$, $k_0 = 0$, and the droplet is homogeneous, with ϕ in the droplet either everywhere positive or negative. If $a < 0$, $k_0 = \sqrt{|a|/b}$, and the droplet is modulated with wavelength $w = 2\pi\sqrt{b/|a|} \ll \xi$, with alternating regions of positive and negative ϕ. Note that w, unlike the twin width, is due to competition between the two gradient terms, because the surface term is negligible near the spinodal for systems with long-range interactions and the bulk term primarily determines the orientation. These predictions apply at early times near the spinodal. During the growth of the martensite phase, the surface will eventually sharpen and twinning will be restored [9].

One of our main goals is to simulate martensites as realistically as possible. To this end, we need to relate the dimensionless simulation parameters in Eq. (1) to empirically accessible parameters. By extending the potential in Ref. [11] to include a second gradient term, the three-dimensional (elastic) free energy near the critical temperature in terms of measurable quantities is

$$F[\epsilon_3] = \int_0^L d^3r\Big[\frac{C_1}{2}\epsilon_1^2 + \frac{C_2}{2}\epsilon_2^2 + \frac{C_3}{2}\epsilon_3^2 - \frac{C_4}{4}\epsilon_3^4 + \frac{C_6}{6}\epsilon_3^6 + \frac{\kappa_1}{2}(\vec{\nabla}\epsilon_3)^2 + \frac{\kappa_2}{4}(\nabla^2\epsilon_3)^2\Big], \tag{5}$$

where a_0 is the crystal lattice spacing, L is the linear dimension, C_1 through C_6 are elastic constants, and κ_1/a_0^2 and κ_2/a_0^4 are strain-gradient coefficients in units of $\mathrm{N/m^2}$. To minimize finite size effects, $L/a_0 \gg \xi$. The parameters in Eq. (5) can be determined empirically [11]. We can approximate the [110] acoustic phonon dispersion curve $\omega(k)$ from neutron scattering at small k by a Taylor expansion in ϕ, $\rho_0\omega^2 = a_2k^2 + gk^4$, where ρ_0 is the mass density. The coefficient a_2 is determined from the slope and is proportional to the corresponding elastic constant C_3 and, therefore, τ [21–23]. The coefficient g is determined from the curvature and is proportional to the strain-gradient coefficient κ_1/a_0^2 and, therefore, a [23]. Including the strain-gradient term in the dispersion implies a nonlocal effective elastic constant and a sound velocity that depends on the magnitude and direction of $\vec{k}$. This method can, in principle, be extended to include the nonlinear and higher order gradient terms in the free energy [24].

We scale all the elastic constants by $A_0 = 9C_4^3/(128C_6^2)$ and the strains by $\epsilon_0 = \sqrt{3C_4/(4C_6)}$ to make the two martensite minima of the homogeneous part of F in Eq. (1b) near unity, and scale all distances by a_0. We define the dimensionless variables $\tilde{\vec{r}} = \vec{r}/a_0$, $\tilde{L} = L/a_0$, $\tilde{F} = F/(A_0a_0^3)$, $e_{1,2} = \epsilon_{1,2}/\epsilon_0$, $\phi = \epsilon_3/\epsilon_0$, $A_{1,2} = C_{1,2}\epsilon_0^2/A_0$, $\tau = C_3\epsilon_0^2/(2A_0)$, $a = 2\kappa_1\epsilon_0^2/(A_0a_0^2)$, and $b = 2\kappa_2\epsilon_0^2/(A_0a_0^4)$.

To find the proper scaling for the time, the noise, and the temperature, we use the Langevin equation for $\epsilon_3(\vec{r}, t)$, which is Eq. (3) with $\phi \to \epsilon_3$, $F[\phi] \to F[\epsilon_3]$, and an explicit friction coefficient γ multiplying the time derivative. The dimensionless time and noise are $\tilde{t} = A_0a_0t/(L\gamma\epsilon_0^2)$ and $\tilde{\zeta} = L\epsilon_0\zeta/(A_0a_0)$. The factor of L is a result of going from $\epsilon_3(x, y, z, t)$ to $\phi(x, y, t)$. The fluctuation-dissipation relation Eq. (4) requires that $\theta = k_BT/(A_0a_0^3)$. θ_c and θ_0 are defined similarly with T replaced by T_c, the critical temperature, and T_0 is the temperature at which the three minima of the homogeneous part of F in Eq. (5) are degenerate. Note that we can change the effective temperature of the simulations by changing either T or a_0. We drop all tildes in the following.

To discretize the Langevin equation, we used a simple forward Euler method [25] for the time derivative. Higher

order algorithms take more time and give similar results. The noise ζ is found by multiplying the standard deviation of the noise σ_ζ by a random number chosen from a Gaussian distribution with unit variance, $G_{i,j,\alpha}$ [25]. On the lattice $\delta^2(\vec{r}-\vec{r}') \approx 1/\delta x^2$ and $\delta(t-t') \approx 1/\delta t$, so $\zeta(\vec{r},t) \approx \sigma_\zeta G_{i,j,\alpha}$, where $\sigma_\zeta = \sqrt{2\theta/(\delta x^2 \delta t)}$.

The nonlocal term in the Langevin equation that arises from Eq. (1e) is a convolution with $\hat{K}(\vec{k}) = \int d^2\rho U(\vec{\rho}) e^{-|\vec{\rho}|/R} e^{-i\vec{k}\cdot\vec{\rho}}$. $\hat{K}(\vec{k})$ needs to be computed only once. The factor $e^{-|\vec{\rho}|/R}$ is computed with the origin at the center of the lattice. The indices i and j correspond to x and y, l and m correspond to k_x and k_y, and α corresponds to t. We write $\phi(x,y,t) \to \phi_{i,j,\alpha}$, $\hat{U}(k_x,k_y) \to \hat{U}_{l,m}$, $e^{-|\vec{\rho}|/R} \to \mathrm{E}_{i,j}$, and $\hat{K}(k_x,k_y) \to \hat{K}_{l,m} \approx \mathcal{F}[\mathrm{E}_{i,j}\mathcal{F}^{-1}(\hat{U}_{l,m})]$, where $\mathcal{F}$ and $\mathcal{F}^{-1}$ represent fast Fourier transforms. The convolution integral is computed as

$$\int_0^L d^2r' U(\vec{\rho}) e^{-|\vec{\rho}|/R} \phi(\vec{r}',t) \approx \mathcal{F}^{-1}[\mathcal{F}(\phi_{i,j,\alpha})\hat{K}_{l,m}]. \quad (6)$$

The accuracy of our algorithm requires treating both spatial derivatives to fourth order in δx, including cross terms in $\nabla^4\phi$. If we define $\oplus^{(1)}_{i,j} = \phi_{i+1,j} + \phi_{i-1,j} + \phi_{i,j+1} + \phi_{i,j-1}$, $\oplus^{(2)}_{i,j} = \phi_{i+2,j} + \phi_{i,j+2} + \phi_{i-2,j} + \phi_{i,j-2}$, and $\otimes_{i,j} = \phi_{i+1,j+1} + \phi_{i+1,j-1} + \phi_{i-1,j+1} + \phi_{i-1,j-1}$, then

$$\nabla^2\phi_{i,j} \approx \frac{1}{12(\delta x)^2}[-\oplus^{(2)}_{i,j} + 16\oplus^{(1)}_{i,j} - 60\phi_{i,j}], \quad (7a)$$

$$\nabla^4\phi_{i,j} \approx \frac{1}{(\delta x)^4}[\oplus^{(2)}_{i,j} - 8\oplus^{(1)}_{i,j} + 2\otimes_{i,j} + 20\phi_{i,j}]. \quad (7b)$$

We use $T_c = 268$ K, $T_0 = 290$ K, and $A_2 = 2A_1$, for all our simulations; these values correspond to FePd [11] so that our simulations are as realistic as possible. We take $L = 64$, $\delta x = 0.05$, and $\delta t = 0.01$ and choose the values of t, a, and b so that the numerical solution is stable. Our solutions were checked for accuracy by comparing the simulation results to the exact analytical solution for the linear case without the noise and nonlocal terms. Numerical stability of the complete equation of motion was checked by varying δt and δx. We chose a and b so that $G \approx 5$ and $\xi \approx 16 = L/4$. We chose $A_1 < 1$ so that the core of the droplet will be more visible. We varied the nucleation rate primarily by changing a_0.

For $a > 0$ we take $a = 6.32$, $b = 0.01$, $R = 6.4$, $\tau = 6.17 \times 10^{-3}$, $A_1 = 1 \times 10^{-3}$, and $a_0 = 2.1544 \times 10^{-8}$ m. FePd has a crystal lattice spacing of ≈ 3 Å, so this value of a_0 corresponds to a coarse-graining factor of 70 and sample size of about 1.38 μm. The value of τ corresponds to $T = 268.14$ K, and a corresponds to $\kappa_1/a_0^2 = 2.79 \times 10^9$ N/m^2. The value of a is reasonable compared to the value of 2.5×10^{10} N/m^2 for FePd quoted in Ref. [11].

For $a < 0$ we take $a = -1.61$, $b = 0.652$, $R = 4$, $\tau = 0.5$, $A_1 = 0.6$, and $a_0 = 2.7 \times 10^{-8}$ m. These values correspond to the modulation wavelength $w \approx 4$, $\tau_s = 0.496\,95$, $T = 279$ K, and $\Delta\tau = 3.048 \times 10^{-3}$.

We begin the simulation with $\phi(\vec{r})$ chosen at random about the metastable austenite minimum at $\phi = 0$. In a short time, $\phi(\vec{r})$ equilibrates at the chosen temperature. On a much longer time scale, the thermal noise causes a critical droplet to appear. By looking at the evolution of the spatial average, $\langle\phi^2(t)\rangle$, we can estimate the nucleation time. In Fig. 1 we see that the system went from a metastable state with $\langle\phi^2\rangle \approx 0$ to the stable state with $\langle\phi^2\rangle \approx 1$ at the time $t = 2430$. Because we expect the amplitude of the droplet to be close to that of the metastable phase, we expect the nucleation time to be prior to the rapid increase in $\langle\phi^2\rangle$.

To determine the nucleation time more precisely, we use an intervention technique [26]. Because the nucleation droplet is a saddle point [8,26], the droplet has equal probability of growing to the stable state or disappearing if we perturb the system at the nucleation time. We use this saddle point property to find the nucleation time. We restart the simulation at the estimated nucleation time, and integrate the equations of motion using a new sequence of random numbers for the noise. Our criterion is that if 8 ± 4 of the 16 runs with different random number sequences show that $\langle\phi^2\rangle$ grows at roughly the same time as in the original run, then the intervention time is equal to the nucleation time. We then look at snapshots of ϕ to see if we can identify the droplet.

For $a > 0$, the nucleation time is $t_n^+ = 2356 \pm 35$, as in Fig. 1. A snapshot of ϕ at $t = 2356$ is shown in Fig. 2(a). Although only the core of the droplet is visible above the noise, the droplet is homogeneous, as predicted.

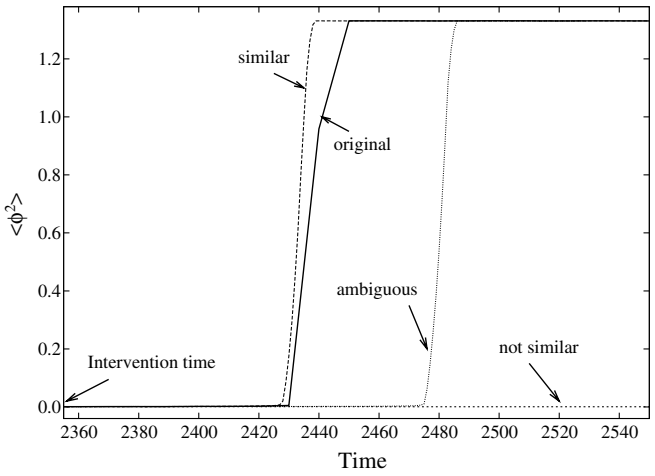

FIG. 1. Evolution of $\langle\phi^2(t)\rangle$ for $a > 0$; the original run and three interventions at $t = 2355$. $\langle\phi^2(t)\rangle$ of the original run grows rapidly from its metastable value to its stable value at $t \approx 2430$. If the intervention run is similar to the original run, the same droplet is assumed to have grown; otherwise, it is assumed that the same droplet did not grow. Some interventions are ambiguous. In this run the intervention time of 2355 is close to the estimated nucleation time of $t_n^+ = 2356 \pm 35$.

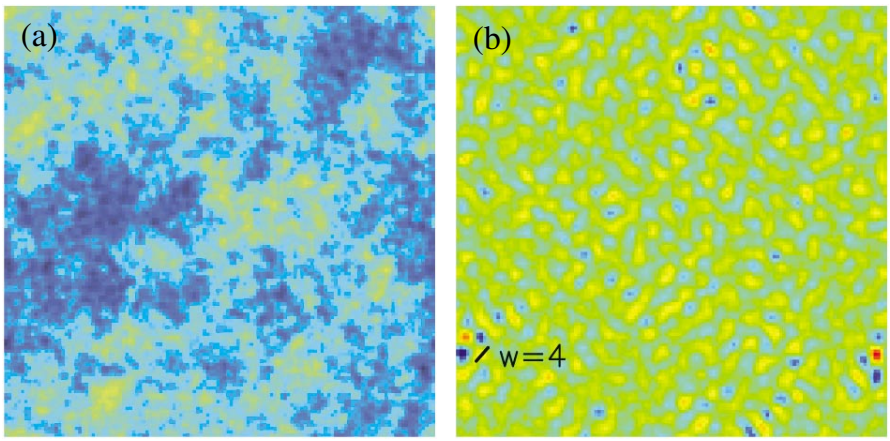

FIG. 2 (color). From left: (a) The deviatoric strain ϕ for $a > 0$ at $t_n^+ = 2356$. The amplitude of ϕ ranges from -0.08 (dark blue) to 0.025 (yellow). The part of the droplet visible above the noise is clearly homogeneous, showing no modulations between the two low temperature minima (red and blue). (b) The deviatoric strain ϕ for $a < 0$ at $t_n^- = 1236.5$. The amplitude of ϕ ranges from -0.2 (dark blue) to 0.2 (red). In the part of the droplet that is visible, the modulations between the low temperature minima (red and blue) have the wavelength $w \approx 4$ predicted by Ref. [13].

For $a < 0$, the nucleation time is $t_n^- \approx 1236.5 \pm 1.5$. The error in t_n^- is much less than for $a > 0$ because the slower growth in $\langle \phi^2 \rangle$ for $a < 0$ makes fewer of the interventions ambiguous. A snapshot of the field at $t = 1236.5$ is shown in Fig. 2(b). As predicted in Ref. [13], the droplet has modulations with wavelength $w \approx 4$. This modulation is different from the twinning in the stable phase which occurs at wavelength $\lambda \sim \sqrt{L} = 8$ [10].

Our results are important for nucleation in many materials with long-range interaction in which strain couples to another physical variable, e.g., polarization in ferroelectrics, magnetization in magnetoelastics, and other multiferroics. We found that for elastic systems the description of nucleation is subtle because of the presence of bulk-interface elastic compatibility constraints that are manifested as long-range interactions.

In summary, when the austenite is quenched to near the pseudospinodal, the structure of the nucleation droplet differs from the structure of the stable martensite phase. If the curvature of the phonon dispersion curve at small k is positive, then $a > 0$, and the droplet is homogeneous. If the curvature is negative, then $a < 0$, and the droplet is modulated by a wavelength w. Our parameters are consistent with austenite to martensite transitions in FePd. Hence, we conclude that the classical nucleation picture is not applicable to these transitions and the spinodal nucleation scenario is a better approach for understanding these transitions.

C. J. G. thanks Daniel Blair for his assistance with Fig. 2, G. R. Barsch for helpful conversations, and LANL and ASU, where some of this work was done. W. K. acknowledges support from the ASC Materials Modeling Program at LANL. The work at LANL was supported by the U.S. Department of Energy.

*Permanent Address: Department of Physics and Center for Computational Science, Boston University, Boston, MA 02215, USA.

[1] A. Borgenstam, Mater. Sci. Eng. A **273**, 425 (1999).
[2] Z. Nishiyama, *Martensitic Phase Transformations* (Academic Press, New York, 1978).
[3] R. Oshima *et al.*, Metall. Trans. **19A**, 803 (1988).
[4] G. B. Olson and A. L. Roitburd, *Martensite*, edited by G. B. Olson and W. S. Owen (ASM International, Metals Park, OH, 1992), Chap. 9.
[5] A. C. E. Reid, G. B. Olson, and B. Moran, Phase Transit. **69**, 309 (1999).
[6] B. P. Van Zyl and R. J. Gooding, Metall. Mater. Trans. **27A**, 1203 (1996).
[7] G. B. Olson and M. Cohen, Metall. Trans. **7A**, 1897 (1976).
[8] C. Unger and W. Klein, Phys. Rev. B **29**, 2698 (1984).
[9] W. Klein and F. Leyvraz, Phys. Rev. Lett. **57**, 2845 (1986).
[10] S. R. Shenoy *et al.*, Phys. Rev. B **60**, R12 537 (1999); T. Lookman *et al.*, Phys. Rev. B **67**, 024114 (2003).
[11] S. Kartha *et al.*, Phys. Rev. B **52**, 803 (1995).
[12] D. W. Heermann *et al.*, Phys. Rev. Lett. **49**, 1262 (1982).
[13] W. Klein *et al.*, Phys. Rev. Lett. **88**, 085701 (2002).
[14] W. Klein, Phys. Rev. E **64**, 056110 (2001).
[15] J. S. Langer, Ann. Phys. (N.Y.) **41**, 108 (1967).
[16] J. Yang *et al.*, J. Chem. Phys. **93**, 711 (1990).
[17] F. J. Cherne *et al.*, Model. Simul. Mater. Sci. Eng. **12**, 1063 (2004).
[18] A. Saxena *et al.*, Physica (Amsterdam) **239A**, 18 (1997).
[19] C. J. Gagne *et al.* (to be published).
[20] P. M. Chaikin and T. C. Lubensky, *Principles of Condensed Matter Physics* (Cambridge University Press, Cambridge, U.K., 2000), Chap. 2.
[21] M. Sato *et al.*, J. Phys. F **12**, 2117 (1982).
[22] N. W. Ashcroft and N. D. Mermin, *Solid State Physics* (Brooks-Cole, Belmont, MA, 1976).
[23] G. R. Barsch and J. A. Krumhansl, Phys. Rev. Lett. **53**, 1069 (1984).
[24] G. R. Barsch and J. A. Krumhansl (to be published).
[25] W. H. Press *et al.*, *Numerical Recipes in Fortran* (Cambridge University Press, Cambridge, U.K., 1992), 2nd ed.
[26] L. Monette and W. Klein, Phys. Rev. Lett. **68**, 2336 (1992).